ENVIRONMENTAL SOFTWARE

Volume 7 1992

Elsevier Applied Science

Development of confidence interval estimates for predictions from a rainfall-runoff model

T. V. Hromadka

Boyle Engineering, 1501 Quail Street, Newport Beach, California 92658-9020, USA

R. J. Whitley

Department of Mathematics, University of California, Irvine, California 92717, USA

R. H. McCuen

Department of Civil Engineering, University of Maryland, College Park, Maryland 20742, USA

&

C. C. Yen

Williamson & Schmid, 15101 Red Hill Avenue, Tustin, California 92680, USA

(Received 10 October 1991; final version received 8 May 1992; accepted 12 May 1992)

Abstract

In any rainfall-runoff model, there is uncertainty associated to predictions of runoff. The stochastic integral equation method is used in this paper to represent the history of the rainfall-runoff modeling error as a convolution of model input (effective rainfall in this paper) with a frequency-distribution of transfer function realizations. In prediction, the expected runoff estimate is quantified by use of a distribution of runoff error estimates, each estimate of error based upon a previous experience using the subject rainfall-runoff model. Although this paper focuses upon a simple unit-hydrograph rainfall-runoff model, the principles discussed apply, in generality, to other rainfall-runoff model structures.

1. INTRODUCTION

Almost all rainfall-runoff models in use today produce a single estimate of runoff for a single storm event (Hromadka et al, 1987). This runoff estimate is then used for design or decision-making purposes, and the level of accuracy achieved in the decision-making process depends upon the accuracy of the runoff prediction. Because only a single estimate of runoff is produced by the rainfall-runoff model judgments regarding accuracy in the decision-making cannot be adequately made.

In this paper, a simple quasi-linear rainfall-runoff model is studied with the objective of developing a stochastic runoff modeling error relationship. This error relationship can then be used to quantify the modeling error associated to the subject rainfall-runoff model when applied to a design or hypothetical storm rainfall event.

The modeling error relationship is developed by use of a stochastic integral representation of the error between model-produced runoff and the catchment's measured runoff (Hromadka and Whitley, 1989). Given several storm events, several error realizations result that are then used in a convolution integral setting, producing realizations of the transfer function needed in the stochastic integral (Hromadka and Whitley, 1988).

The catchment rainfall-runoff data used are pairs of associated realizations of "measured" rainfall and runoff, produced by a synthetic physically-based rainfall-runoff model of a hypothetical catchment. Consequently, there is no "measurement error" in the rainfall-runoff synthetic data used in this study. The rainfall information are realizations of synthetically generated rainfalls that are "measured" at a single rain gauge located near the hypothetical catchment. The storm rainfalls are stochastic events with random areal extent, shape, storm patterns, duration, intensities, speed, direction, and approach. The physically-based rainfall-runoff model (discussed in a later section) utilizes a Horton

Environmental Software 0266-9838/92/$05.00

loss function with recoverable initial loss rates, diffusion-based topographic and open channel routing algorithms, and regional non-homogeneity in subarea loss rate parameters. Because the rainfall and runoff data and runoff characteristics are known precisely throughout the catchment, and with respect to the rain gauge, there are no unknown hydrologic processes that can contribute to the modeling error. Thus, the modeling error relationship derived herein focuses upon the discrepancies between model input (rainfall) and output (runoff).

After developing the modeling error relationship associated with the subject quasi-linear rainfall-runoff model, the uncertainty in runoff predictions can be evaluated by coupling the developed error relationship to the estimated single realization of runoff from the calibrated rainfall-runoff model.

II. THE RAINFALL-RUNOFF MODEL

The subject rainfall-runoff model being considered is a single area unit-hydrograph (UH) model. The UH modeling approach continues to be one of the most widely used rainfall-runoff modeling techniques. The methods used in this paper apply to other rainfall-runoff models. An average (UH) is calibrated from the rainfall-runoff data and is the average of all reconstitutions. The loss rate function used is the phi-index scheme (Hromadka et al, 1987), and is also calibrated from the data. The model is described for storm event i by

$$M^i(t) = \int_{s=0}^{t} e^i(t-s)\ \psi^i(s)\, ds \tag{1}$$

where $e^i(\cdot)$ is the estimated storm event i catchment area-averaged effective rainfall; $\psi^i(\cdot)$ is the associated unit hydrograph; and $M^i(t)$ is the model estimate of runoff for storm event i. In (1),

$$e^i(s) = \max\,[(P^i(s) - \phi^i), 0] \tag{2}$$

where $P^i(\cdot)$ is the event i precipitation record "measured" at the rain gauge, and ϕ^i is a constant phi-index. In (1), the rainfall-runoff model is applied to and calibrated from n storm events that are considered significant runoffs.

In the application of Eqs. (1) and (2) for model calibration, a phi-index value of ϕ^i is determined for each storm event i such that the volume of effective rainfall equals the volume of runoff. For n storm events, the calibrated phi-index, ϕ_C, is the sample mean

$$\phi_C(s) = \frac{1}{n}\sum_{i=1}^{n} \phi^i \tag{3}$$

The calibrated UH, $\psi_C(s)$, is the pointwise average of n storm event unit hydrographs, $\psi^i(s)$, i=1,2,...,n, where for each storm event i, $\psi^i(s)$ is determined by equating model estimated runoff, $M^i(t)$, to measured runoff, $Q^i(t)$. (Existence of the $\psi^i(s)$ is assured when effective rainfall initiates at or before measured runoff.) Thus, $\psi_C(s)$ is determined by the mean of realizations

$$\psi_C(s) = \frac{1}{n}\sum_{i=1}^{n} \psi^i(s),\ s\geq 0 \tag{4}$$

The model error for storm event i, $E^i(\cdot)$, is

$$E^i(t) = Q^i(t) - M_C^i(t) \tag{5}$$

where the calibrated model estimate of runoff for event i, $M_C^i(\cdot)$, is

$$M_C^i(t) = \int_{s=0}^{t} e_C^i(t-s)\ \psi_C(s)\, ds \tag{6}$$

and $e_C^i(t) = \max\,[(P^i(t) - \phi_C), 0]$.

The model error is assumed to be correlated to the calibrated catchment-averaged effective rainfall estimate, $e_C^i(\cdot)$, and is equated to the convolution

$$E^i(t) = \int_{s=0}^{t} e_C^i(t-s)\ \eta^i(s)\, ds \tag{7}$$

resulting in n realizations, $\eta^i(\cdot)$; i=1,2,...,n, for the considered n storm events. Other choices for equating model error via convolution is the calibrated model estimate itself, $M_C^i(\cdot)$; the storm measured rainfalls, $P^i(\cdot)$; among others. In this paper, the calibrated-averaged effective rainfall is used to develop estimates of runoff modeling error due to the resulting simplifications in the mathematical model; specifically,

$$Q^i(t) = M_C^i + E^i(t) = \int_{s=0}^{t} e_C^i(t-s)\ \psi^i(s)\, ds \tag{8}$$

where

$$\psi^i(s) = \psi_C(s) + \eta^i(s) \tag{9}$$

The distribution of realizations $\{\psi(\cdot)\}$, is approximated by the set of equally likely realizations, $\{\psi^i(s);\ i=1,2,...,n\}$.

In prediction, the rainfall-runoff model estimate is the

distribution of outcomes, $[M^D(\cdot)]$, for storm event "D", where

$$[M^D(t)] = \int_{s=0}^{t} e_c^D(t-s)\,[\psi(s)]\,ds \tag{10}$$

or in approximation,

$$[M^D(t)] \approx \left\{ \int_{s=0}^{t} e_c^D(t-s)\,\psi^i(s)\,ds;\ i=1,2,\ldots,n \right\} \tag{11}$$

where as before,

$$e_c{}^D(t) = \max\,\{(P^D(t) - \phi_c), 0\} \tag{12}$$

and $P^D(t)$ is the rain gauge rainfalls for event "D".

In the above analysis, no constraints (other than requiring effective rainfalls to exist at or prior to beginning of runoff) are introduced in the development of the various convolution transfer functions. Consequently, both positive and negative values of transfer functions generally result. If it is desired to eliminate negative values of runoff, a filter on the $[M^D(\cdot)]$ realizations may be used that simply restricts all $[M^D(\cdot)]$ realization values to be positive, or otherwise zero, or an interval mean value used defined on the time interval $(t-\delta, t+\delta)$. The distribution, $[M^D(\cdot)]$, as filtered, is hereafter denoted by $[M^D(\cdot)]^*$.

If we are interested in the value of a criterion variable, such as peak flow rate, maximum channel flow depth, average flow velocity during the peak one-hour of flow, or other, a distribution $[A^D]^*$ of values is developed by

$$[A^D]^* = \mathcal{A}[M^D(\cdot)]^* \tag{13}$$

where $[A^D]^*$ is the distribution of filtered values of the criterion variable for hypothetical storm event "D"; $\mathcal{A}$ is notation for operating upon each realization (distributed as $[M^D(\cdot)]^*$) in determining the value of the subject criterion variable for each realization of runoff.

In the subsequent sections of this paper, the above procedures are applied towards developing the various distributions of stochastic processes involved, and estimates of distributions are developed for several criterion variables of typical concern.

III. SYNTHETIC RAINFALL-RUNOFF DATA GENERATION

In order to have a large sample of rainfall-runoff realization sets, a stochastic storm model is used to develop synthetic realization sets of storm rainfall. Storm rainfalls are synthetically generated that are random in areal extent, shape, duration, intensities, velocity, direction, and approach to the test catchment.

Rainfall depths were randomly sampled using probability distributions that are representive of Los Angeles regional rainfall data for the Pacific coastal area. As the synthetic storm rainfalls occur, a single rain gauge (see Fig. 1) "measures" rainfall quantities as they are defined in the vicinity of the rain gauge.

The synthetic catchment model represents a 38 square mile area with the use of a coupled topographic routing model and a channel routing model. The zero inertia (or diffusion) flow routing (Hromadka and Yen, 1987) is used for hydraulic modeling purposes. The topographic model utilizes interconnected grids, each with its own Horton loss function parameters, slope, time-of-concentration, and drainage connection to the channel system. The interconnected channel system network serves to drain the topographic model by use of various channel reach sizes and friction factors. The overall synthetic runoff model represents hydraulic and loss rate characteristics that are typically found in fully urbanized planned-community areas that have open space, office, schooling, and residential areas. The channel system drains to the catchment stream gauge (see Fig. 1).

The synthetic storm rainfall event is modeled by time-stepping, at one-minute intervals, the storm event over the subject catchment pursuant to the various samplings of storm speed, size, areal extent, and other factors. Synthetic runoff is then generated according to the storm rainfall incremental one-minute depths. For each storm event, i, a synthetic rainfall realization and an associated synthetic runoff realization is developed, which is to be subsequently used as the "measured" rainfall-runoff data in calibrating the previously discussed UH model of Eqs. (1) and (6).

IV. COMPUTATION OF TRANSFER FUNCTIONS, $\psi^i(\cdot)$

In Hromadka and Whitley (1988), the UH model transfer function for storm event i, $\psi^i(\cdot)$, is shown to represent the sampling of mutually dependent random variables and random processes by

$$\psi^i(s) = \sum_{j=1}^{m} \sum_{<\ell>} a^P_{<\ell>} \sum_{k} [\lambda^P_{jk}]\,\phi_j{}^P(s - [\theta^P_{jk}] - \alpha^P_{<\ell>}) \tag{14}$$

where

$\psi^i(s)$, is the realization for storm event i;

s = time;

$<\ell>$, is an index sequence of channel segments;

$<\ell>_j$, is the channel segment sequence between subarea j and the stream gauge (Fig. 1);

$a_{<\ell>}$, are convolution coefficients representing channel routing;

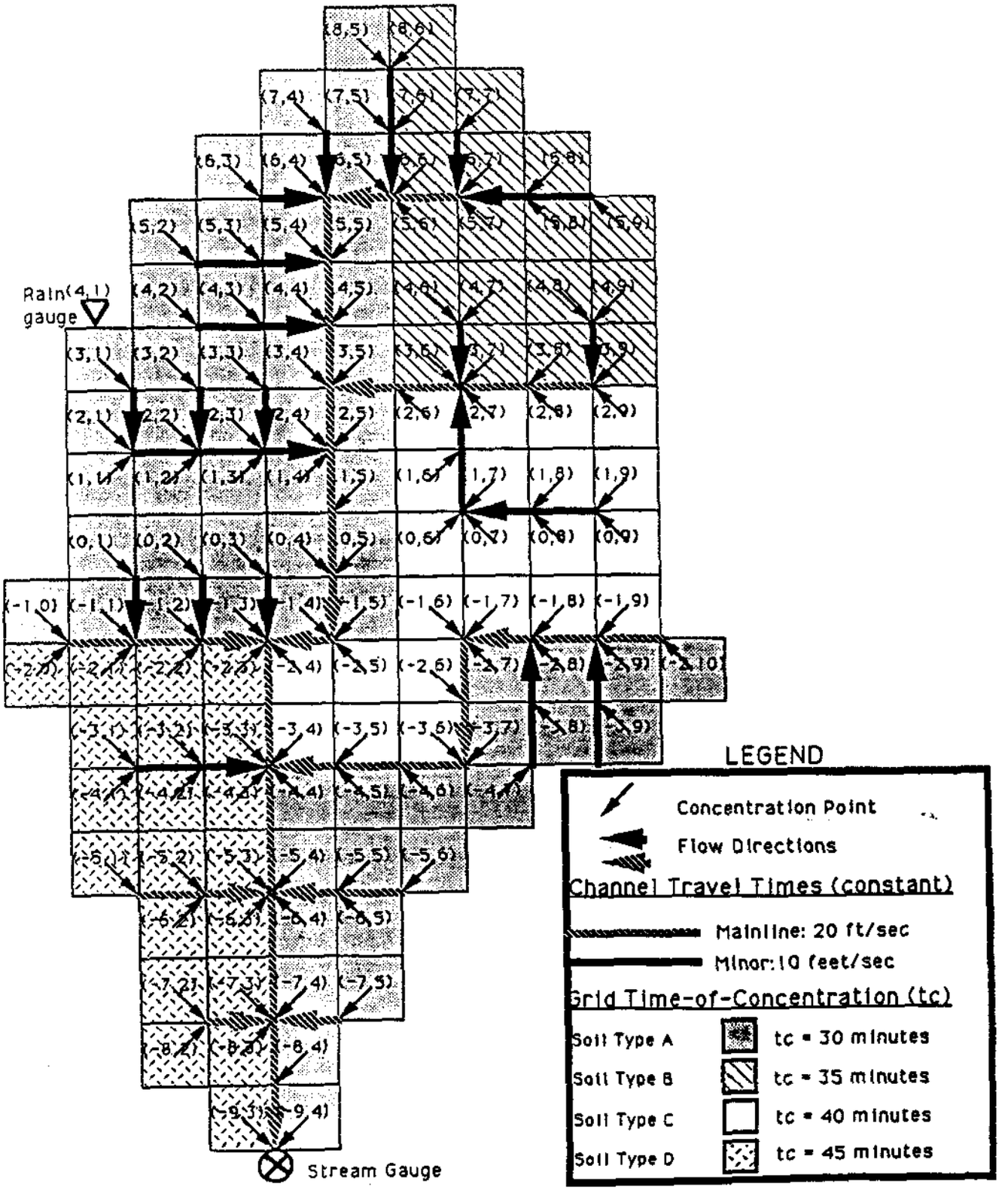

Fig. 1. Simulation Rainfall-Runoff Model Catchment.

P, is a storm class, and introduces nonlinearity effects;

$[\lambda_{jk}]$, are random effective rainfall convolution coefficients in relating subarea effective rainfalls to measured data with respect to the rain gauge;

$\phi_j(s)$ is the subarea j transfer function;

$[\theta_{jk}]$, are random timing offsets used in effective rainfall convolutions;

m is the number of subareas in the link-node model;

$\alpha_{<\ell>}$, are channel routing convolution timing offsets.

In the cited reference, the UH model is used to represent a wide variety of catchment response characteristics. Even though the various random processes and distributions are unknown (given data from only a single rain gauge and stream gauge), the mutual dependency between the random variables and processes are properly represented in the single random realization of $\psi^i(\bullet)$ for each storm event, i. As shown in Hromadka and Whitley (1988), it is incorrect to simply assign plausible distributions for the several random components in Eq. (11) and assume the distributions to be mutually independent (for example, the assumption of independence typically leads to concluding that a decrease occurs in the variance of the distribution $[A^D]$ as the number of model random components, generally associated to the number of subareas "m", increases). Each storm event has an associated vector of samplings for each random component of Eq. (14), and that vector is properly represented by the single realization $\psi^i(\bullet)$.

For each storm event, $\psi^i(\bullet)$ is developed via solving for the inverse convolution as described by Eqs. (7) - (9). Some of the $\psi^i(\bullet)$ realizations obtained by use of the synthetic rainfall-runoff data are plotted in Fig. 2.

The distribution $[\psi^i(\bullet)]$ can be normalized in S-graph form (i.e., summed mass; or cumulative distribution) by use of catchment lag as shown in Fig. 3.

V. *RUNOFF PREDICTION MODEL*

For hypothetical storm event "D", the runoff prediction is probabilistically modeled as the ensemble of runoff hydrograph realizations distributed as $[Q^D(\bullet)]$ approximated by

$$[Q^D(\bullet)] \approx \{M_k^D(\bullet);\ k=1,2,...,n\} \tag{15}$$

where n is the number of storm events available in the data set (in this paper, n=50); and as before,

$$M_k^D(t) = \int_{s=0}^{t} e^D(t-s)\ \psi^k(s)\ ds \tag{16}$$

The $M_k^D(\bullet)$ realizations may be filtered to remove negative values, or some other smoothing method applied.

For a selected criterion variable, A, (such as peak flow rate, or detention basin maximum volume anticipated, and so forth), the prediction is probabilistically approximated by the frequency distribution, $[A^D]$,

$$[A^D] \approx \{\mathcal{A}(M_k^D(\bullet));\ k=1,2,...,n\} \tag{17}$$

In Eq. (17), a parent probability distribution function (pdf) may be apparent, and can be used in estimating confidence intervals.

It is noted that the various distributions used in Eq. (14) may be dependent upon the severity of storms and that the use of storm classes (e.g., severe, major, mild, minor) may be appropriate. The use of storm classes (Hromadka and Whitley, 1988) introduces a source of nonlinearity in the rainfall-runoff model of Eq. (10) in that the distribution $[\psi^i(\bullet)]$ is conditioned upon the realization of effective rainfall. The cited reference found that storm classes can be developed according to values of specified peak durational effective rainfalls such as (1-hour, 3-hour, 6-hour) values among other choices. Storm classes, however, are not used in this study.

VI. REGIONALIZATION OF THE DISTRIBUTION $\psi^i(\bullet)]$

Two other synthetic catchments were analyzed for the development of other synthetic distributions of transfer functions, $[\psi^i(\bullet)]$. When normalized in S-graph form, the three distributions showed form and shape similarities. (Although each of the three hypothetical catchments was subjected to a sequence of 50 storm events, the storm sequences differed between catchments in that each catchment was subjected to a continuation of the random rainfall event generator rather than a repetition or rearrangement of the 50 storm events.)

Figure 4 depicts a weighted S-graph representation of the three separate catchment results in developing distributions $[\psi^i(\bullet)]$. The 8 weighted realizations are developed as a simple population mean weighted among similar S-graphs, each S-graph shown being the computed average of a particular grouping of S-graphs. It is recalled that Fig. 4 represents the ensemble of S-graphs developed from three catchments.

In Fig. 4, the S-graph distribution is normalized with respect to the expected S-graph, i.e., the calibrated UH. The S-graph weighted realizations are plotted in units of percentage of expected lag.

The discretized regional distribution for $[\psi^i(\bullet)]$, shown in Fig. 4, may be assumed to apply at other catchments, for the subject rainfall-runoff model of Eq. (10). Should an

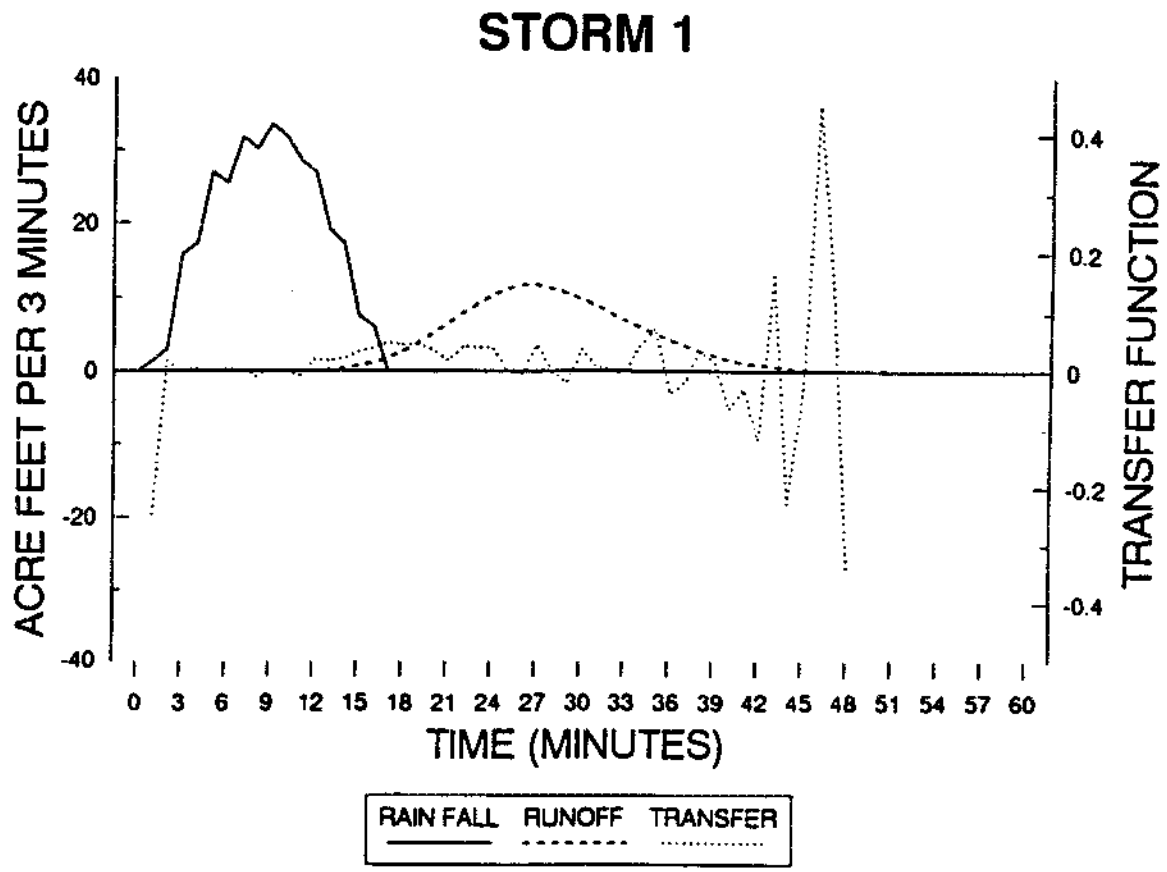

Fig. 2a. Transfer Function for Storm #1.

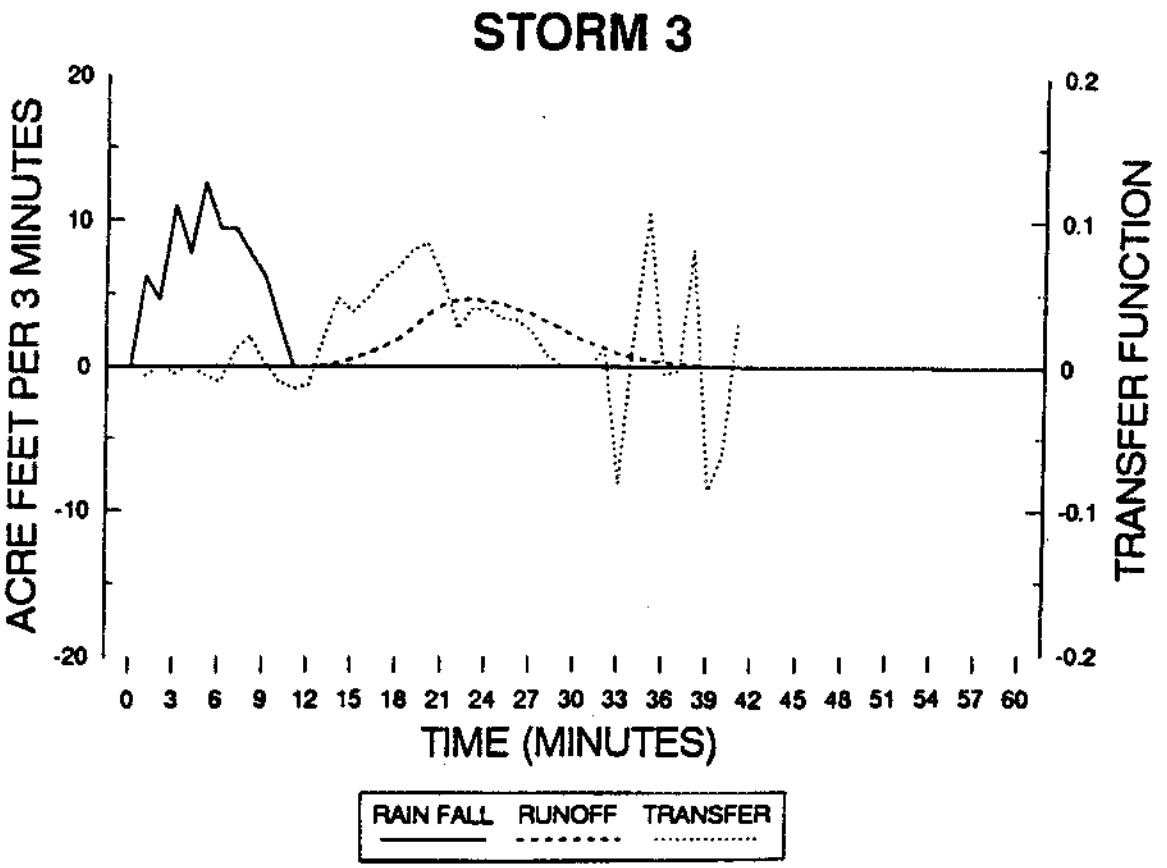

Fig. 2b. Transfer Function for Storm #3.

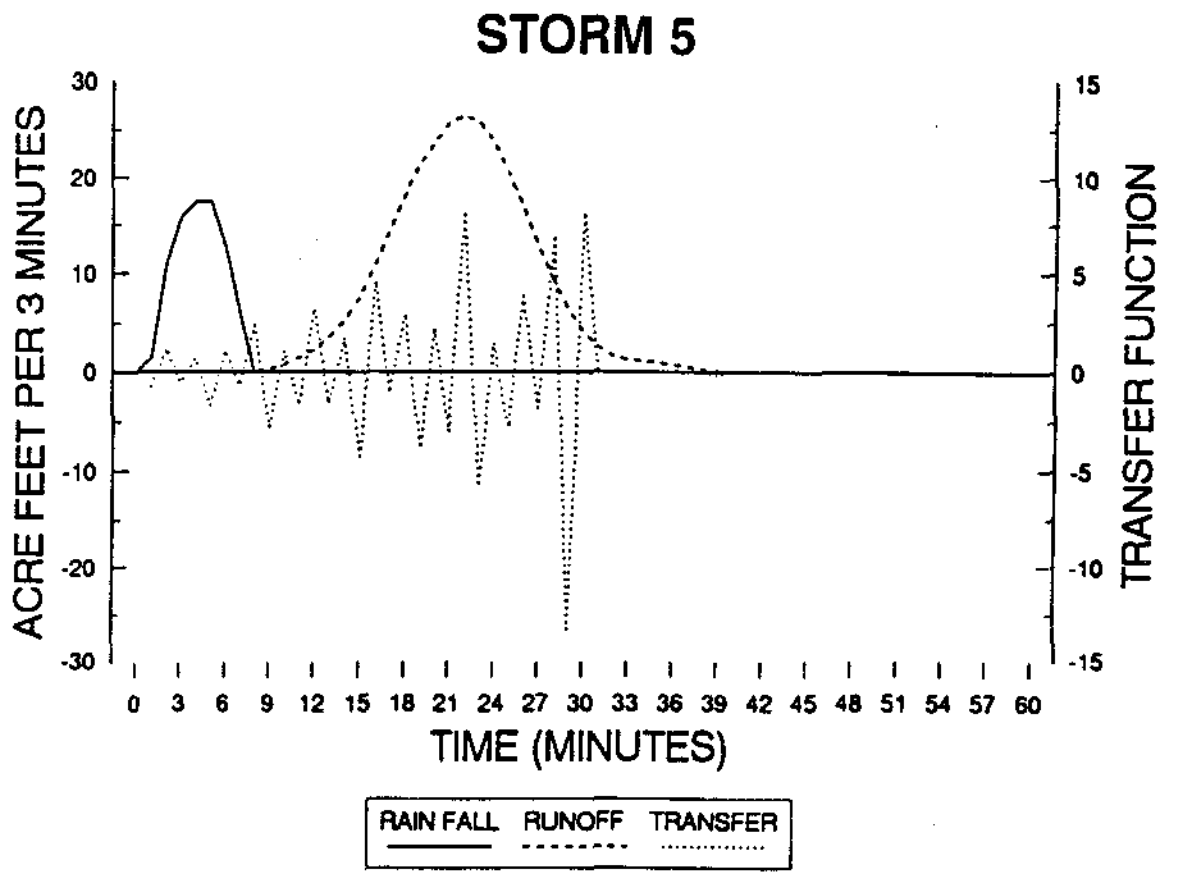

Fig. 2c. Transfer Function for Storm #5.

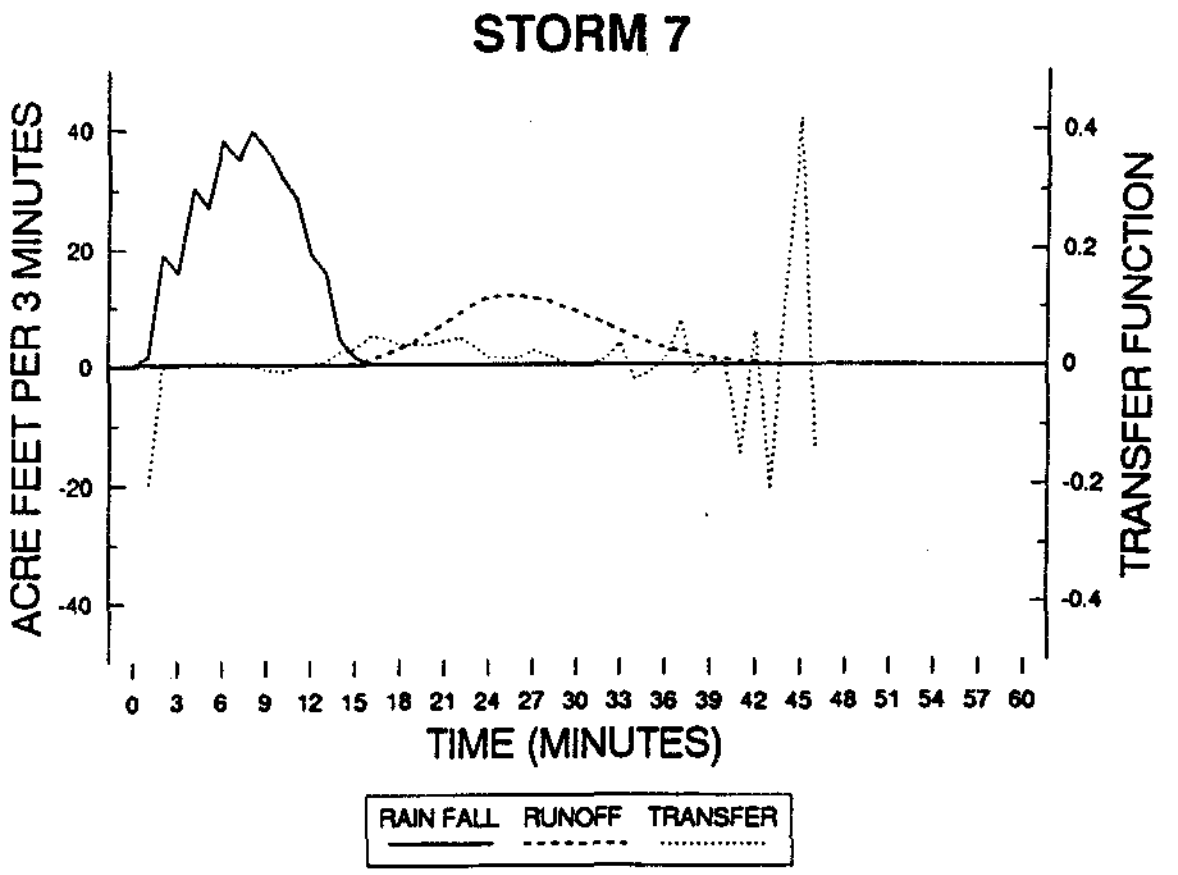

Fig. 2d. Transfer Function for Storm #7.

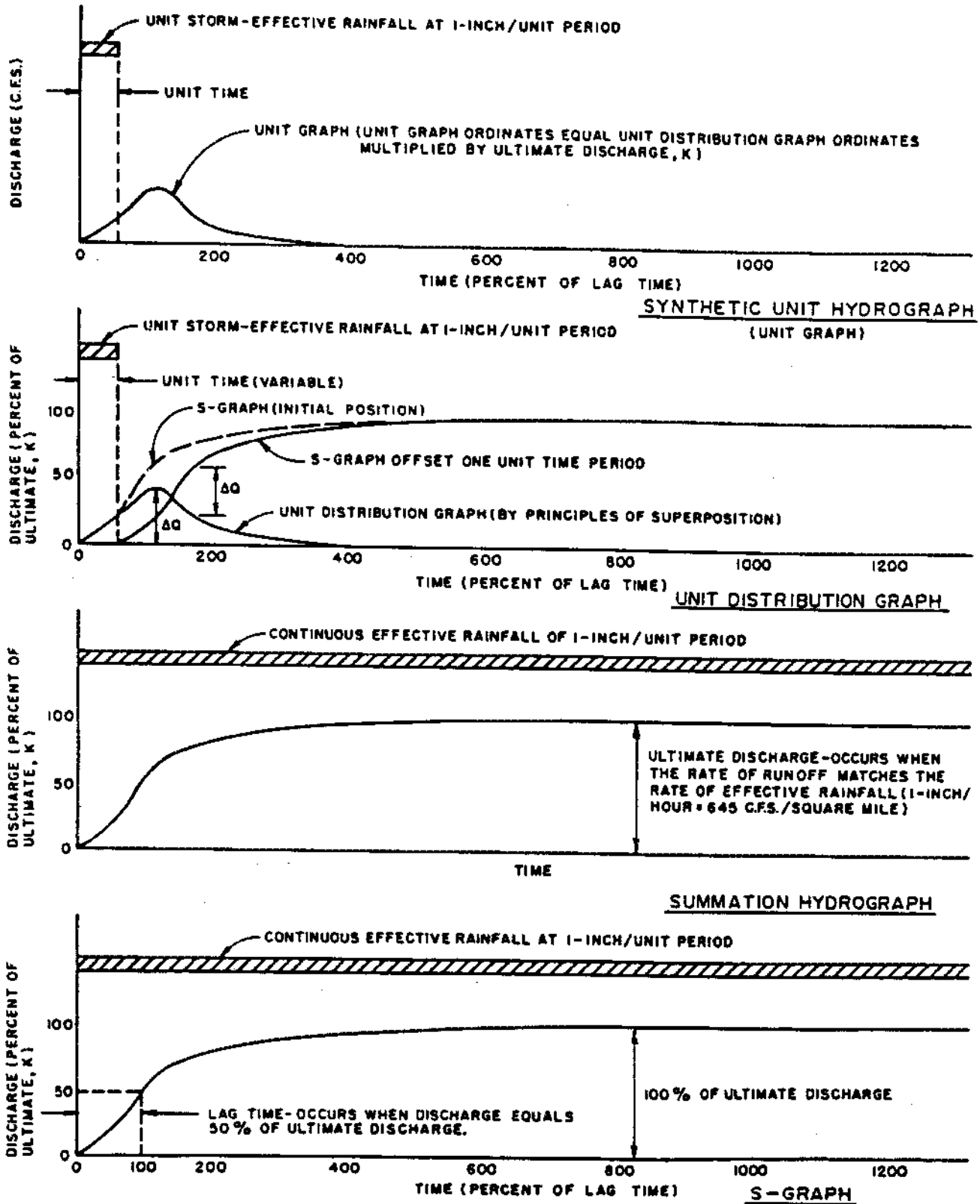

Fig. 3. Relationship Between Transfer Function (Unit-Hydrograph), S-Graphs, and Lag.

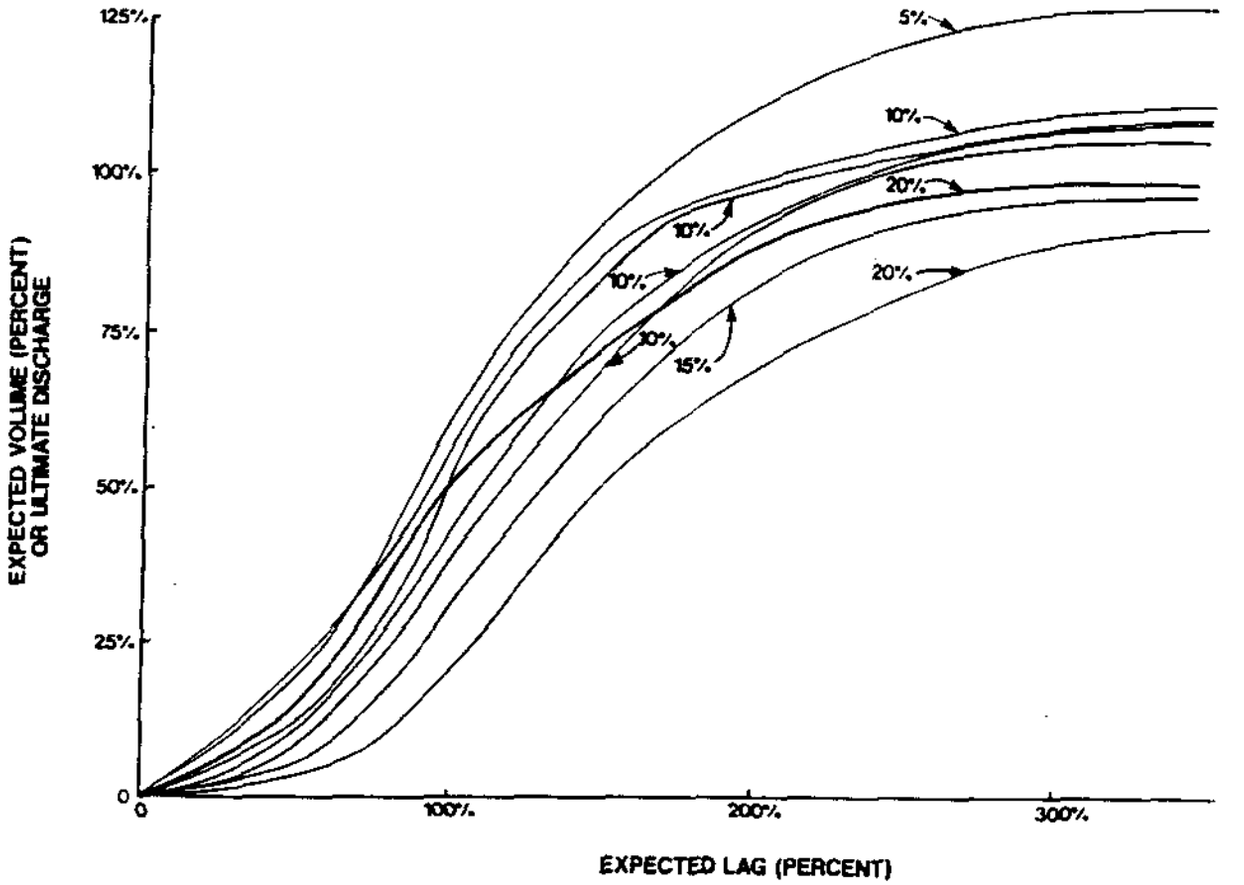

Fig. 4. Regionalized Frequency-Distribution Weightings of S-Graphs. The Expected S-Graph is shown in heavy line.

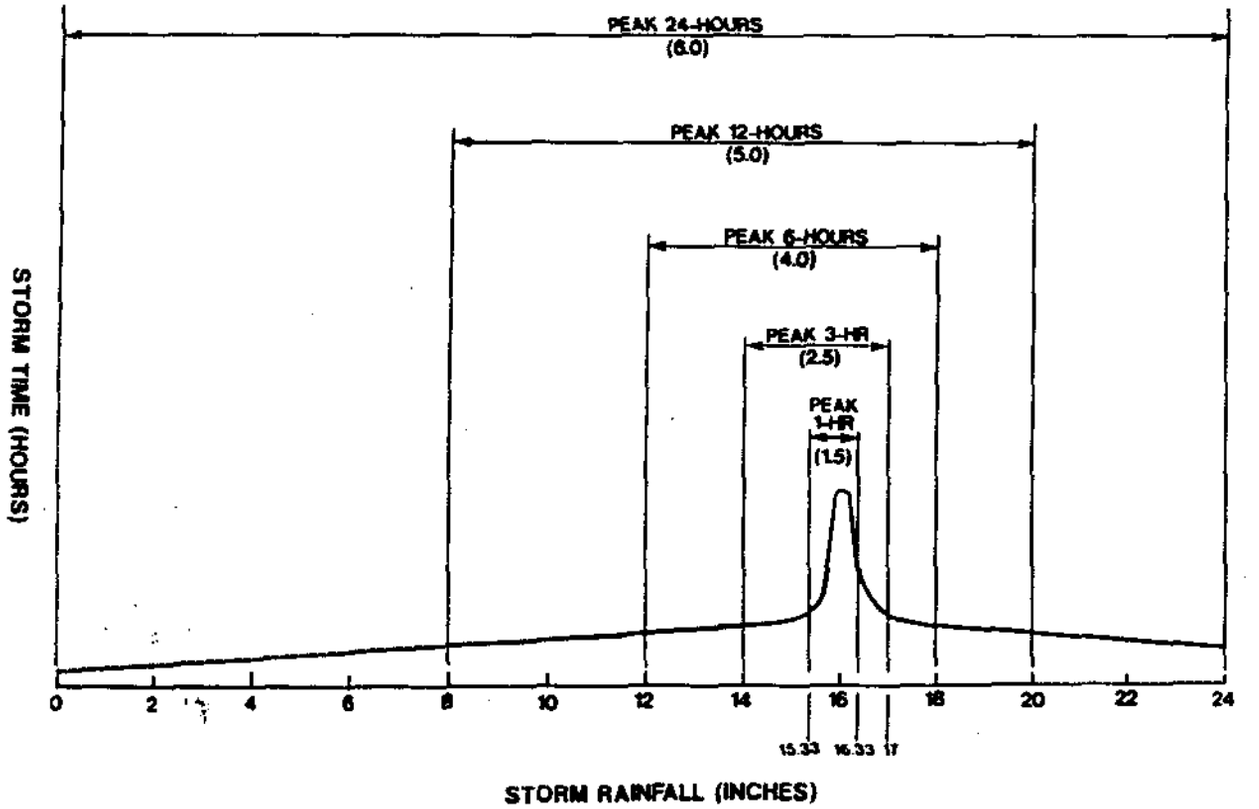

Fig. 5. Hypothetical Rainfall Pattern and Depths (Inches).

estimate for expected lag be available, such as obtained from commonly used generalized regression equations (e.g. McCuen and Snyder, 1986), the $[\psi^i(\bullet)]$ distribution may be estimated by scaling the frequency-distribution of Fig. 4. It is noted that the distribution, $[\psi^i(\bullet)]$, lacks the full breadth of realizations needed for sampling rare events. However, use of $[\psi^i(\bullet)]$ in evaluating a runoff criterion variable aids in identifying an underlying distribution of the criterion variable, $[A^D]$.

VII. APPLICATION OF THE REGIONAL DISTRIBUTION, $[\psi^i(\bullet)]$, IN EVALUATING UNCERTAINTY IN RUNOFF ESTIMATES

The application of Eqs. (10) and (11) in estimating distributions for runoff criterion variables, by Eqs. (13) and (17), is considered below. In each example application, the rainfall-runoff model previously calibrated is applied to a catchment not included in the calibration set (i.e., the three synthetic catchments used to develop $[\psi^i(\bullet)]$. The study catchment has an area of 3000 acres, an expected lag of 1.0 hours, and an expected phi-index of f = 0.4 inch/hour. The hypothetical rainfall event, $P^D(t)$, is shown in Fig. 5.

Peak Flowrate Estimate

The criterion variable of peak flow rate is estimated for event $P^D(t)$, by the distribution

$$[Q_p] = \mathcal{A}[M^D(\bullet)]^* \tag{18}$$

where $\mathcal{A}$ is the operator that, for sample $M^k(\bullet) \in [M^D(\bullet)]^*$,

$$\mathcal{A}(M^k(\bullet)) = \max_{t \geq o} M^k(t) \tag{19}$$

Table 1 provides the weighted peak flow rate estimates computed by use of the 8 weighted realizations in Fig. 4. A frequency-distribution of peak flowrate estimates, using the previously developed synthetic $[\psi^i(\bullet)]$, is shown in Fig. 6. Superimposed in Fig. 6 is a normal distribution $n(\hat{\mu}, \hat{\sigma})$, where $\hat{\mu}$ and $\hat{\sigma}$ are the estimated sample mean and

TABLE 1. PEAK FLOW RATE ESTIMATE

Realization (see Fig. 4)	Weighting	Peak Flow (cfs)
1	10	3094
2	20	2485
3	15	1630
4	10	1664
5	10	2423
6	20	2771
7	10	1782
8	5	1847

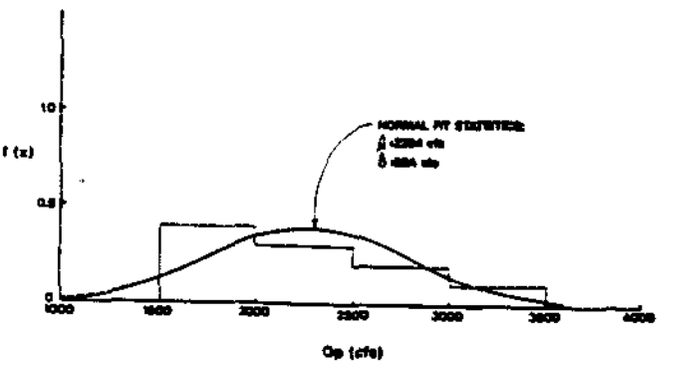

Fig. 6. Frequency Distribution of $[Q_p]$.

standard deviation values weighted according to the frequency-distribution weightings of $[\psi^i(\bullet)]$. (The normal distribution is shown for illustration purposes only, and is not intended to suggest that $[Q_p]$ is normally distributed.)

Reduction in Peak Flow Rate Due to Channel Routing Storage Effects

There are many unsteady flow routing models reported in the literature (e.g., McCuen, 1989). One commonly used hydrologic routing model is the Convex method (McCuen, 1989). In this application, the change in peak flow rate ΔQ_p, due to the channel storage effects as predicted by the Convex routing method is of interest. A Convex coefficient of C = 0.75 is used in the application, for a channel of two-mile length.

For each weighted realization shown in Fig. 4, a runoff hydrograph is developed for the considered design storm, $P^D(t)$, resulting in 8 weighted runoff runoff hydrographs, $\{M^k(t), k=1,2,...,8\}$. Each $M^k(t)$ is then routed by the Convex method, and ΔQ_p noted. Table 2 summarizes the results. Figure 7 depicts a frequency-distribution of ΔQ_p, for the computed information, and a normal distribution using estimates $\hat{\mu}$ and $\hat{\sigma}$ is also shown. In this application, $[A^D] = [\Delta Q_p{}^D]$, where superscript D

TABLE 2. ΔQ_p ESTIMATE DUE TO CONVEX CHANNEL ROUTING

Realization (see Fig. 4)	Weighting	ΔQ_p
1	10	55
2	20	120
3	15	56
4	10	103
5	10	387
6	20	152
7	10	86
8	5	61

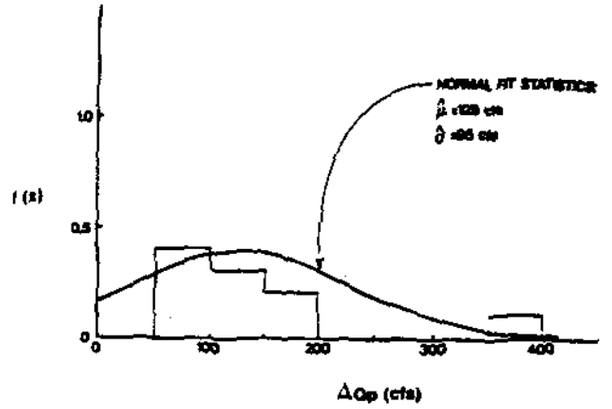

Fig. 7. Frequency Distribution of $[\Delta Q_p]$ due to Convey Channel Routing.

refers to the hypothetical or design storm event of Fig. 5. With respect to the A operator of Eq. (13), $\mathcal{A}$ is the process of identifying the ΔQ_p associated to a sampled transfer function from the distribution $[\psi^i(\cdot)]$.

Estimation of Maximum Detention Basin Volume Demand

The estimate of maximum runoff volume needed to be stored in a detention basin is a critical design parameter. Using the Fig. 4 information, the estimate of basin volume demand can be developed.

The subject detention basin has a single pipe outlet with no downstream hydraulic backwater effects. Using a modified Puls storage routing calculation, the weighted maximum basin volume demands are provided in Table 3. As in the previous examples, the frequency-distribution for basin maximum volume and a normal $n(\hat{\mu}, \hat{\sigma})$ distribution is shown in Fig. 8.

Estimate of Mean Flow Velocity for Maximum One-Hour Duration of Runoff

In sedimentation analysis, a mean flow velocity, usually above some threshold value, is of interest. In this

TABLE 3. ESTIMATE OF MAXIMUM VOLUME DEMAND

Realization (see Fig. 4)	Weighting	Maximum Volume (AF)
1	10	123
2	20	87
3	15	20
4	10	22
5	10	34
6	20	117
7	10	32
8	5	47

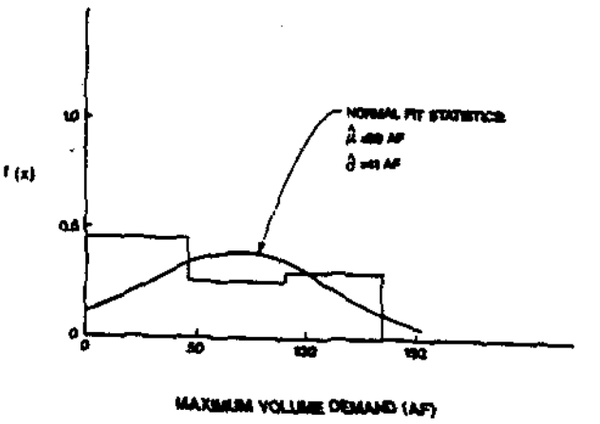

Fig. 8. Frequency Distribution of Maximum Volume Demand.

application, the variation in mean flow velocity estimates corresponding to the maximum one-hour duration of flow is computed. An economical channel section composed of sandy material is considered. A Manning's friction factor of n = .035 is assumed for the channel. Table 4 and Figure 9 depict the computed information.

TABLE 4. MEAN FLOW VELOCITY FOR MAXIMUM ONE-HOUR ONE-HOUR DURATION OF RUNOFF

Realization	Weighting	Mean Velocity (fps)
1	10	5.3
2	20	5.1
3	15	4.6
4	10	4.5
5	10	4.6
6	20	5.2
7	10	4.6
8	5	4.8

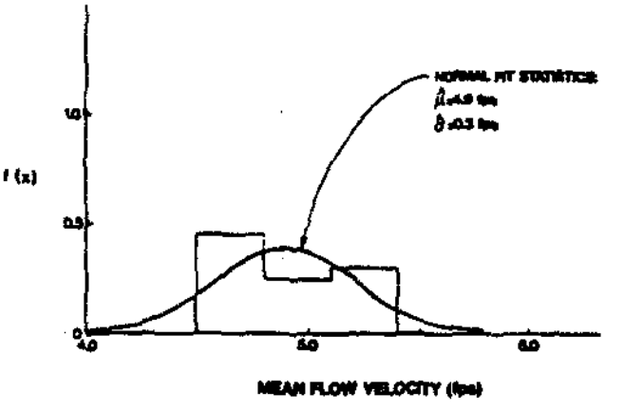

Fig. 9. Frequency Distribution of Mean Flow Velocity for Maximum One-hour Duration of Runoff.

VIII. DISCUSSION OF RESULTS AND CONCLUSIONS

In any rainfall-runoff model, there is uncertainty associated to predictions of runoff. The stochastic integral equation represents a history of modeling error as a convolution of model input (effective rainfall in this paper) with a frequency-distribution of transfer function realizations. In prediction, the expected runoff estimate is qualified by a distribution of runoff error estimates, each estimate of error based upon a previous experience using the subject rainfall-runoff model.

For a selected criterion variable (such as peak flow rate, detention basin volume, etc.), the prediction is not a single value but instead is a frequency-distribution of values that may be used to estimate confidence intervals for safety in design and planning. For example, one may select to be 85-percent confident in a design value for sizing storage in a detention basin as associated to a prescribed design storm event, $P^D(\cdot)$.

As with any statistical estimation procedure, accuracy hinges upon the quantity and quality of the data used in the synthesis. Consequently, with rainfall-runoff data in short supply, one may elect to supplement the available data by use of a stochastic rainfall-runoff synthetic runoff information generator such as employed in this paper. It is recalled that considerable data are necessary when attempting to estimate the high confidence interval estimates (e.g., 95%).

Although this paper focuses upon a simple unit-hydrograph (UH) rainfall-runoff model, the principles discussed apply to any rainfall-runoff model structure in generality (see Hromadka and Whitley, 1989). The UH method is particularly tractable to use of the stochastic integral formulation due to the summation of the transfer function distribution to the expected UH, resulting in a single stochastic integral equation.

Many questions arise when developing distributions for the various criterion variables of usual interest. For example, what is the underlying distribution for peak flow rate estimates; or for peak one-hour durational flow mean velocity; or for detention basin maximum volume demand? How much data is needed to adequately define the underlying distribution parameters? What confidence level should be used for design purposes? These questions, among others, require further research and a considerable collection of environmental data.

REFERENCES

1. Hromadka II, T.V., and Whitley, R.J., Stochastic Integral Equations and Rainfall-Runoff Models, Springer-Verlag, 1989, ISBN 0-387-51086-9.
2. McCuen, R.H., Hydrologic Analysis and Design, Prentice-Hall, 1989, ISBN 0-13-447954-8.
3. Hromadka II, T.V., McCuen, R.H., Yen, C.C., Computational Hydrology in Flood Control Design and Planning, Lighthouse Publications, 1987, ISBN 87-080497.
4. McCuen, R.H., Snyder, W.M., Hydrologic Modeling: Statistical Methods and Applications, Prentice-Hall, 1986, ISBN 0-13-448119-4.
5. Hromadka II, T.V., and Whitley, R.J., The Design Storm Concept in Flood Control Design and Planning, Stochastic Hydrology and Hydraulics, Vol. 2, pp. 213-239, 1988.
6. Hromadka II, T.V., and Yen, C.C., A Diffusion Hydrodynamic Model (DHM), U.S. Geological Survey Special Report 87-4137.